Numerical simulation of slope stability and landslides under different loadings in the Karongi district, western Rwanda

By

Sylvain Barayagwiza

Supervised by: Professor Catherine Meriaux and
Professor Alberto Armigliato

A thesis submitted in partial fulfilment of the requirements for the award of a Master's degree in Geophysics

International Center for Theoretical Physics- East African Institute for Fundamental Research (ICTP-EAIFR)

February 21, 2025

The degree is submitted in full fulfillment
The TURNITN anti-plagiarism check declaration

DECLARATION

I declare that this thesis is my original work and has not been submitted previously for any degree at the University of Rwanda or any other institution. All sources used have been acknowledged appropriately.

Student: Sylvain Barayagwiza

UR Registration Number: 222021479

Supervisors: Professor Catherine Meriaux

Professor Alberto Armigliato

Dedication

This thesis is dedicated to my lovely wife, who has been my biggest strength with her unwavering support and encouragement; to my parent, whose guidance and sacrifices shaped my journey; and to my friends, whose companionship and inspiration have been so valuable in this journey.

Acknowledgement

I am deeply grateful to my supervisors, Prof. Catherine and Prof. Alberto, for their immense amount of useful advice, encouragement, insightful feedback, continuous support and expertise provided during this research.

I must extend my special thanks to the Rwanda Space Agency for availing essential topographic data and to the Ministry of Agriculture and Animal Resources for the geotechnical dataset. I also appreciate the Earthquake Catalog from the U.S. Geological Survey for facilitating seismic data analysis.

I am profoundly grateful to the International Center for Theoretical Physics (ICTP) - East African Institute for Fundamental Research (EAIFR) for arranging all aspects of my study, and to the Government of Rwanda for generously sponsoring my education.

I am, therefore, grateful to my family and friends for their patience and encouragement during this challenging journey. Lastly, my genuine appreciation to the University of Rwanda for fully equipping me with the knowledge and means to undertake this thesis.

Abstract

Slope stability and landslides are significant threats to human life, infrastructure, and socio-economic activities in the Karongi District of Western Rwanda, which is characterized by steep slopes, heavy rainfall, and seismic activity. It is very important to understand the dynamics of slope stability under variable conditions of loading for effective disaster mitigation and sustainable land management. This study investigates slope stability and landslide susceptibility under such conditions. Using the Limit Equilibrium Method (LEM), Scoops3D software, and QGIS for the analysis, high-resolution Digital Elevation Model (DEM), pore water pressure ratios, seismic forces, and detailed land use information are integrated in simulating and analyzing slope behavior. The findings of this study provide a better understanding of the strong influences of pore water pressure ratios, seismic activity, and land cover on slope stability. The higher pore water pressure ratios tend to decrease the Factor Of Safety (FOS) values, indicating the vital role of pore water pressure in increasing the slope instability. Similarly, the model representing areas with proximity to roads, bare or agricultural lands are most prone to instability. Slope instability in susceptible areas was exacerbated by seismic loading, which in this case was represented by a Peak Ground Acceleration (PGA) of 0.065g. Historical landslide data allowed the validation of the model, hence showing the reliability of identifying high-risk zones. The validation of the model's predictive capability at the Karongi region based on the historical landslide data in eastern DRC, Rwanda, and Burundi within 2000-2019 shows quite good correspondence of historical landslide locations with areas with FOS less than 1.0. Notably, the model highlighted a horseshoe-shaped zone in the southeastern part of Karongi district that had shown low FOS values, with no recorded historical landslides. This area comprises bare ground with very little vegetation cover and thus is very susceptible to slope failure, particularly at high pore water pressure ratios. The present findings emphasize that predictive modeling for latent landslide risk is important; therefore, the area requires detailed geotechnical investigation and mitigation strategies in a proactive approach. These results identify potential uses of this model in early warning systems and disaster mitigation strategies. The research puts forward a step in understanding slope stability dynamics in high-risk regions and gives practical insights into sustainable land management and disaster risk reduction.

Contents

1 Introduction

Slope stability is one of the critical concerns in geophysics and geotechnical engineering, particularly in the areas that are historically prone to landslides due to complex interactions between geological, meteorological, and seismic factors [1, 2, 3]. Landslides are among the most destructive natural hazards defined as the down-slope movement of rock, earth, or debris under the direct influence of gravity that poses significant threats to human lives, infrastructure, environment and socio-economic activities such as agriculture and urban development[1, 4]. The triggering factors can turn out to be responses to quite different kinds of natural causes: heavy rainfall, snowmelt, or other water sources can saturate the ground, reducing its stability and leading to landslides; seismic activity can trigger landslides by shaking the ground, allowing water to infiltrate layers, and causing them to slide[5]; and geological formations; supplemented by anthropogenic ones like deforestation, urbanization, infrastructure such as roads construction and unproper land use [6, 1]. These issues complicate the development of reliable landslide prediction models and early warning systems, particularly in low-capacity regions that are highly vulnerable to landslide impacts [7].

The complex nature of the mechanisms, caused by such interacting factors in landslides and logical analysis of slope stability to select proper countermeasures has traditionally been one of the most interesting matters for geologists, engineers, geophysicists and environmental scientists. In its essence, understanding of slope stability under excess load and rainfall is among the crucial elements in disaster risk reduction, promoting effective mitigations in areas prone to landslides [8]. These landslides, becoming more frequent and intense in many parts of the world-tropical and mountainous regions alike-reinforce the imperative necessity for comprehensive studies that integrate field data, geomatic tools, physical modelling and advanced statistical methods while assessing landslide susceptibility to inform policy-making for sustainable land management [6, 9].

Like other tropical parts of the world, in western Rwanda, steep slopes, high rainfall, and active tectonic settings combine to contribute the area most vulnerable to slope failures and landslides. The central part of western Rwanda, Karongi district is the region most affected by landslides[10]. The understanding of slope stability under varying environmental conditions will be important in developing mitigation strategies that enhance disaster resilience in this region [11]. Numerical simulations are an important part of the geophysical investigations for slope stability, as they may have a potential to give information on the triggering and the mechanisms of landslide events[12]. In general, integration of meteorological and seismic data by a numerical model enables an overall assessment of the slope behavior under real-world conditions [13, 14]. This research will employ topographic data like Digital Elevation Method(DEM), subsurface conditions about material properties, Earthquake loading and configuration of groundwater to develop accurate simulations related to slope stability in the central Western Rwanda, Karongi district. The Limit Equilibrium Method

specifically Bishop's Simplified Method and Ordinary(Fellenius) Method, will be employed to analyze the slope stability under coupled meteorological and seismic forcing with subsurface conditions. The methods can provide a trustworthy way of assessing slope stability by the balance between the driving and resisting forces along the potential slip surfaces.

2 Literature Review

2.1 Slope Stability Factors

Slope stability is influenced by a combination of geological, hydrological, and the physical environmental factors. A landslide occurs when the forces resisting slope movement, shear strength are smaller than the forces driving the slope to fail (shear stress), such as gravity[15]. In the tropical regions of seasonal intense rainfall, like Rwanda, this is considered a major triggering factor of landslides since it increases the pore water pressure and reduces soil strength by changing the hydrodynamics of a slope [2]. The seismic activity can trigger landslides with or without it causing sudden failure of slopes. By shaking the ground, allowing water to infiltrate layers, and causing them to slide[5, 3].

2.2 Numerical Modeling of Slope Stability

Numerical modeling has become a standard way to analyze slope stability for different conditions. Finite Element Method (FEM) is widely used to discretize the mechanical behavior of slopes under stress [12]. This method can incorporate complex boundary conditions and material properties, thus providing a detailed analysis of slope response to external forces. Incorporating topographic data, such as DEM into simulations provide more precise presentation of slope geometry and variation in terrain[11, 10]. Information on subsurface conditions, the properties of various soils and rock layers, form an important part of evaluating strength and stability characteristics of slopes under different loading conditions [14]. As long as the groundwater configuration affects the pore water pressures inside the slope, it becomes another critical factor in slope stability. Accurate modeling of subsurface and hydrological conditions in numerical models is crucial for predictions of landslide occurrences under both meteorological and seismic forcing.

2.3 Limit Equilibrium Method (LEM) in Slope Stability Analysis

Limit Equilibrium Method (LEM) is the most widely used of all methods for slope stability analysis, because it is quite simple and effective to practice the

balance of forces along a potential slip surface[16]. Bishop's Simplified Method is the approach that deals with the moment equilibrium of forces acting on a slope and assumes a circular slip surface. However, this method can get more accurate results for slopes whose homogeneous material properties [17]. While the Ordinary-Fellenius Method is simpler and less precise for slopes of variable material properties, it provides a basic equilibrium analysis by considering the overall balance of forces [18].

2.4 Application of LEM in Previous Studies

Several studies have highlighted the application of LEM in slope stability analysis. For instance,[13] , combined LEM with GIS-based models in order to assess the susceptibility to landslip, taking into account rainfall and seismic information for areas of Vietnam that have similar climatic and geological conditions to those in western Rwanda. Using LEM, [14] simulated the combined impacts of meteorological and seismic factors in evaluating the slope stability conditions. This showed the potential of such approaches to the analysis of complicated slope conditions. Western Rwanda is basically characterized of a complex geological setting with a majority of volcanic soils and steep terrain highly predisposing its topography to landslides [10]. There is high precipitation in the region, with incidences of heavy rainfall during rainy times between March and May and from September to November [19]that highly contributes to slope instabilities[11]. The country is also part of the East African Rift System, characterized by active tectonics, implies that it is possible to feel an earthquake at any time [20]. This situation, together with the heavy rainfall posed in this region, makes slope stability challenging.

2.5 Landslide Susceptibility Mapping in Rwanda

Several investigations have been carried out recently in an attempt to map landslide susceptibility in Rwanda, using various methodologies. For instance,[11] applied statistical and machine learning techniques toward the identification of highly landslide-prone areas in western Rwanda. Their results have brought forward that incorporation of causal factors such as meteorological and seismic factors into assessments of slope stability would provides better predictive performance.

The study by [10] presents an advanced landslide susceptibility mapping in Western Rwanda using a number of advanced techniques that include artificial neural networks, frequency ratio, and Shannon entropy models. The main results of this study reveal that geology, rainfall, slope degree, and elevation with proximity to rivers significantly influence the occurrence of landslides in this western part of Rwanda. This study integrated high-resolution spatial data with machine learning and statistical models to produce landslides susceptibility maps. On the other hand, it lacks the integration of physical-based slope

stability analysis using LEM, such as Bishop's Simplified and Ordinary Methods, presented in this study. This leaves a very critical gap in the research that needs consideration in future studies. Despite the advances that have been made, both in understanding slope stability and mechanisms causing landslides in Western Rwanda, there is still a problem of accurate landslide forecasting, especially under different forcing factors. Advanced numerical models need to be integrated with topography, rainfall, soil properties, and seismic activity data with an accurate resolutions.

2.6 Importance of Factor of Safety (FOS) in Slope Stability Analysis

The Factor of safety (FOS) is the most important factor in the stability analysis of slopes and landslides; it is a dimensionless ratio of resisting forces against driving forces along a potential slip surface [15]. The factors influencing the FOS include soil properties such as cohesion, angle of internal friction, and unit weight; groundwater conditions; and external forces such as seismic loading and high rainfall[15]. In the present study typically in western Rwanda, these factors were not directly assessed by using LEM, and analyses of material properties and groundwater configurations in 3D, which are very crucial in making valid predictions of slope stability for both static and dynamic conditions.

2.7 Incorporating 3D Analysis in Slope Stability

With the inclusion of LEM in 3D soil and groundwater configuration analyses, this study provides an all-rounded approach toward slope stability in Western Rwanda. This method not only allows for the calculation of the FOS but also enhances understanding of the internal and external interactions driving slope behavior under various environmental conditions, hence improving the predictive accuracy of landslide hazard assessments as identified by [10].
This work tries to meet these challenges by applying the Limit Equilibrium Method (i.e. Bishop's Simplified Method and the Ordinary Method detailed in chapter 3) to the analysis of slope stability under the combined forcing of meteorological and seismic agents, using detailed topography data (DEM), subsurface conditions, and groundwater configurations in Western Rwanda. The result will provide insight into the likely cause of the forcing of landslide occurrences in the area and will be useful in suggesting the formulation of specific mitigation strategies.

2.8 Application of Scoops3D in Slope Stability Analysis

The application of Scoops3D (See section 3.1.1 for more detail) on slope stability analysis under various load conditions has been done in a wide range of studies. In Vietnam, for example, the integration of the limit equilibrium method with

geospatial data for slope stability analysis within changes due to rainfall was approached by using Scoops3D[21]. This served to model landslide scenarios that could be used for early warnings and urban planning. In Japan, seismic stability after the 2018 Hokkaido Eastern Iburi earthquake was well analyzed using Scoops3D, which showed capability in predicting landslide susceptibility within pyroclastic deposits[22]. Then, the model was validated with a coseismic landslide inventory from which good efficiency has been emphasized for disaster mitigation purposes.

In China, the Scoops3D coupled with the InSAR technique was applied for dynamic assessments of landslide susceptibility during impoundment of the reservoir of the Baihetan dam[2]. It integrated stability coefficients from Scoops3D with geotechnical parameters and real-time slope displacement data to provide an effective and timely response against environmental changes. The catastrophic flank collapse of stratovolcanoes could be reviewed by using Scoops3D, as shown in the analysis of Mount St. Helens[23]. In the present research, the primary assessment of slope stability was conducted using the software Scoops3D and a subsequent probabilistic assessment was made using a hybrid model of an artificial neural network and firefly algorithm[23]. This combination provides an effective estimation of the probability of failure in seismic and non-seismic conditions. These examples illustrate the flexibility and performance of Scoops3D across a wide range of geohazard situations from rainfall-induced and seismic-triggered landslides, through volcanic rock failures. Hence, it becomes an indispensable tool in landslide risk assessment and mitigation.

2.9 Research questions:

Although much knowledge on slope stability and landslide mechanisms is continuously being made in Western Rwanda, accurate forecasting in the perspective of combined meteorological and seismic loading remains difficult. In most studies, the physical-based slope stability methods like the Limit Equilibrium Method have not been fully integrated into the assessment of landslide susceptibility. Such an analysis demands detailed topography data, subsurface soil characteristics, and dynamic factors such as seismic activities.
This study will try to bridge such gaps through the following research questions:

1. How do the slopes of the highlands influence landslides?
2. How do the land cover and land use influencing landslides occurence?
3. How do groundwater configuration affect slope stability in the Karongi District
4. How does seismic loading influence landslides in the Karongi district, Western Rwanda?

3 Methodology

This Chapter presents the research data and methodology adopted for modeling slope stability and landslides in various loading conditions in the Karongi district. A detailed discussion is carried out about the study area, the tools and techniques applied, soil and geotechnical parameters considered in the analysis, and assumptions during the simulation process. This approach embodies a comprehensive methodology that incorporates geoinformatics, numerical simulation models, and geotechnical assessments to ensure completeness in the approach toward landslide risks in the region.

3.1 Basic principles: Material and methods.

Materials and methods applied in this study to analyze slope stability in the Karongi District will be discussed here. These include the Limit Equilibrium Method in its formulations known as Ordinary (or Fellenius) and Bishop's Simplified methods, and tools like DEM, QGIS, and Scoops3D for simulating slope stability and processing data in this research.

3.1.1 The Limit Equilibrium Method and the Scoops3D software

The Limit Equilibrium Method (LEM) is used to analyze the stability of a slope by computing the Factor of Safety (FOS). The FOS is the ratio of the resisting forces - that is, the shear strength - to the driving forces - that is, the shear stress acting along a potential failure surface. This is represented mathematically as:

$$FOS = \frac{\text{Resisting Forces (Shear Strength)}}{\text{Driving Forces (Shear Stress)}} \tag{3.1}$$

$$FOS = \frac{S}{\tau} \tag{3.2}$$

Where:
- S = average shear resistance (strength) along the failure surface,
- τ = shear stress required to maintain limit equilibrium [24].

Based on the definition, a slope is considered stable if FOS > 1 and unstable if FOS < 1.

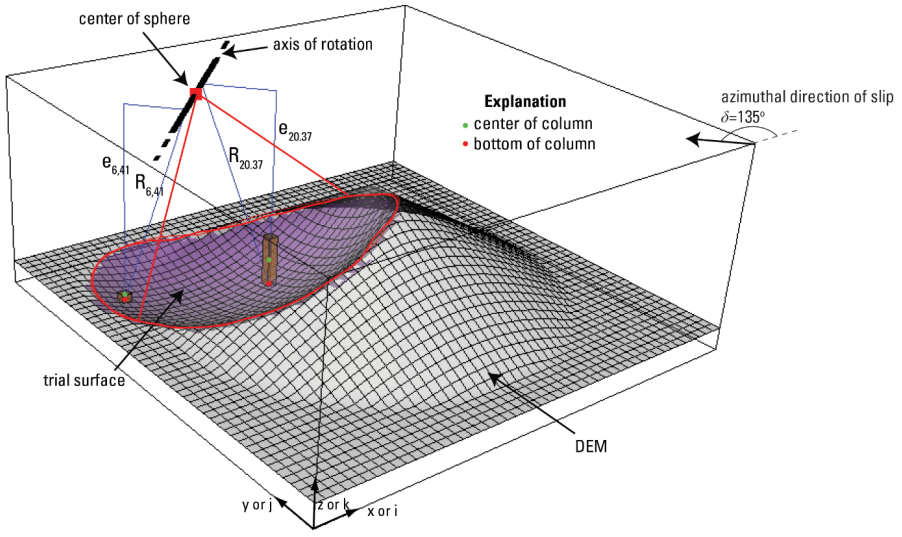

Figure 1: 3-D view of a cone-shaped DEM with a potential failure surface[24].

Figure 1 shows a 3D perspective view of a cone-shaped DEM and one possible trial failure surface. The potential failure mass (extract in this figure) is composed of an assemblage of columns that are defined by the DEM grid. The center of the spherical trial surface and the axis of rotation are located above the DEM. Two columns are colored in brown The distances from the column base to the axis of rotation, $R_{i,j}$, are presented for each column; i,j is the DEM cell location. Horizontal earthquake loading, if selected by the user, is applied to the center of the columns and uses the vertical distance from the rotational axis ($e_{i,j}$), in the limit-equilibrium calculations [24]. The upper right gives the azimuthal direction of slip, perpendicular to the axis of rotation, δ.

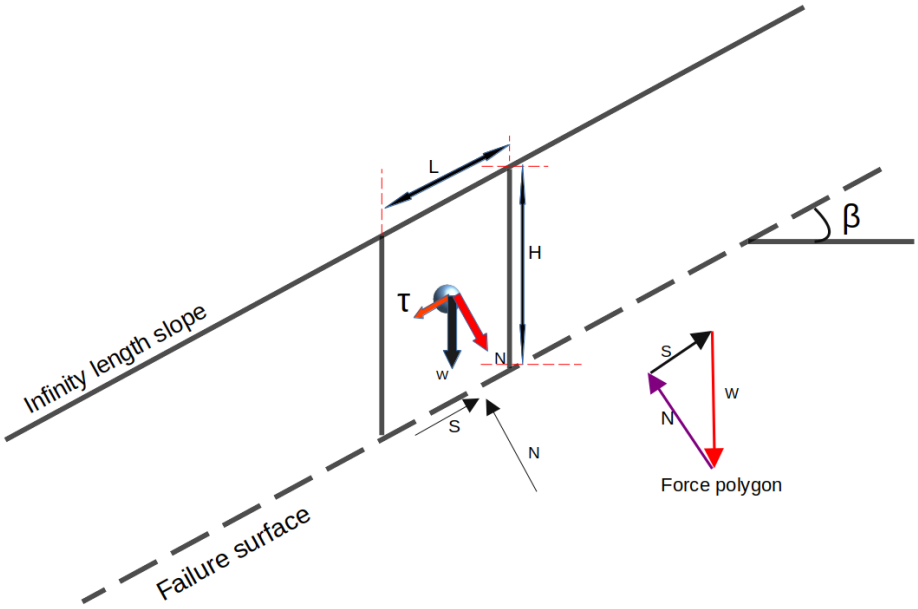

Figure 2: Schematics of slip direction and forces on a column: The weight W, normal force N, resisting shear force S, the shear stress τ applied at the column center.

$$\tau = W \sin \beta \tag{3.3}$$

$$N = W \cos \beta \tag{3.4}$$

In slope stability analysis, shear strength (S) along a potential slip surface is expressed by the Coulomb-Terzaghi failure criterion[24] that calculates the shear strength as a function of cohesion (c), angle of internal friction (ϕ), normal stress (N) and pore-water pressure (u). The general form of this law may be written as:

$$S = c + (N - u) \tan \phi \tag{3.5}$$

$$FOS = \frac{c + (N - u) \tan \phi}{W \sin \beta} \tag{3.6}$$

where β is the slope angle (see Figure 2). In the very simple assumption that cohesion (c) and pore-pressure (u) are zero, then

$$FOS = \frac{(W \cos \beta) \tan \phi}{W \sin \beta} \tag{3.7}$$

$$FOS = \frac{\tan \phi}{\tan \beta} \tag{3.8}$$

This over-simplified expression shows that as the angle of internal friction ϕ increases, FOS also increases while the increase of slope angle decreases FOS. To get a first rough idea of the values of ϕ that may lead to instability, we mention that according to [25] in Rwanda the minimum angle for slope instability is 14°, which is largely exceeded by the average slope angle of 35° characterizing the Karongi district.
In this research, FOS calculations are carried out through Scoops3D, an open source software provided by the United States Geological Survey (USGS, https://www.usgs.gov/software/scoops3d), The software models slope stability under various conditions, including purely gravitational and seismic loading. With reference to Figure 1 (which coincides with Figure 2.1 in [24]), Scoops3D divides the potential failure mass into vertical 3D columns, each of which is assumed to be a rigid mass undergoing no internal deformation. The upper surfaces of the columns are part of the topographic profile of the studied area, while the lower bases are part of the failure surface that in Scoops3D is a portion of a sphere. LEM estimates the stability of the mass by computing the balance of forces and torques in each column (see Figure 2). It can be demonstrated that, in the most general case, the number of equations that are obtained by imposing the equilibrium of forces and torques is less than the number of unknowns. A number of different approaches to solve this problem has been proposed since the 50's of the past century. In the balance of the forces, a critical role is played by the inter-column forces. Scoops3D implements two possible choices, leading to the so-called Ordinary (or Fellenius) Method and Bishop's Simplified Method.

1. **Ordinary (Fellenius) Method** This method assumes a circular failure surface and the Factor of Safety determined by comparing moments of resisting and driving forces without including any inter-column forces. While easy to compute, this method tends to be very conservative, i.e. on the safe side, in its estimations of slope stability[24]. The equation for the FOS is expressed as:

$$FOS = \frac{\sum R_{i,j}\left[c_{i,j}A_{i,j} + \frac{\cos^2\alpha_{i,j}}{\cos\epsilon_{i,j}}\left(W_{i,j} - k_{eq}W_{i,j}\tan\alpha_{i,j}\right)\left(1 - r_{u_{i,j}}\right)\tan\phi_{i,j}\right]}{\sum W_{i,j}\left[R_{i,j}\sin\alpha_{i,j} + k_{eq}e_{i,j}\right]} \tag{3.9}$$

Where:
- FOS: Factor of safety, indicating the stability of a slope.
- $R_{i,j}$: is the distance from the axis of rotation to the center of the column i,j (used in slope stability analysis).
- $c_{i,j}$: Cohesion of the soil in column i,j, which contributes to the soil's shear strength.
- $A_{i,j}$: is the area of the trial surface at the base of each column i,j.
- $\alpha_{i,j}$: is the apparent dip of the column base i,j in the direction of rotation .
- $\epsilon_{i,j}$: is the true dip of the trial surface at the column base i,j.
- $W_{i,j}$: Weight of the column i,j.
- k_{eq}: is a horizontal pseudo-static acceleration coefficient.

- $r_{u_{i,j}}$: Pore pressure ratio for column i, j, which reduces effective normal stress on the failure plane due to pore pressure.
- $\phi_{i,j}$: Angle of internal friction for the material in column i, j.
- $e_{i,j}$: is the horizontal driving force moment arm for a column i, j (equal to the vertical distance from the center of the column to the elevation of the axis of rotation).
- $A_{h_{i,j}}$: Horizontal area or base area for column i, j.

2. **Bishop's Simplified Method**

   Bishop's Simplified method is an improvement on the Ordinary method as it takes into account normal forces between adjacent columns. Since no inter-column shear forces are assumed to occur, it does calculate the inter-column normal forces that give a more realistic estimate of the Factor of Safety[24]. It is computed iteratively from the following expression:

$$FOS = \frac{\sum R_{i,j} \left[c_{i,j} A_{h_{i,j}} + W_{i,j}(1 - r_{u_{i,j}}) \tan \phi_{i,j} \right] / m_{\alpha_{i,j}}}{\sum W_{i,j} \left[R_{i,j} \sin \alpha_{i,j} + k_{eq} e_{i,j} \right]} \tag{3.10}$$

   Where:

$$m_{\alpha_{i,j}} = \cos \epsilon_{i,j} + \frac{\sin \alpha_{i,j} \tan \phi_{i,j}}{FOS} \tag{3.11}$$

3.1.2 Digital Elevation Model (DEM)

For this study, a 10-m resolution Digital Elevation Model (DEM), was used to capture the topography of Karongi District. DEM forms the basis of slope stability analysis, whereby it provides detailed elevation data that enable computation of slope angles among other terrain-related factors. The resolution of DEM selected here creates a good balance between computational efficiency and the amount of detail needed to capture topographic intricacy within this region. DEM was sourced from Rwanda Space Agency and it was processed in QGIS. The pre-processing included re-projection to the correct coordinate system and cropping to area of interest.
This DEM provides the backbone for geospatial analysis in Quantum Geographic Information System (QGIS) and the slope stability simulations performed in Scoops3D.

3.1.3 QGIS – Data Visualization and Processing

Throughout the whole research, spatial data has been visualized and manipulated using QGIS (https://www.qgis.org), an open source GIS platform. QGIS has been used to process the DEM, as well as other spatial layers of land use and infrastructure, in a format to be read by Scoops3D

software. In support, land use maps were downloaded and added into QGIS, including categories such as, residential areas, forested regions, and roads. These were then layered onto the DEM to analyze how land use intersects with areas of potential slope instability.

Once pre-processed, data were exported from QGIS in formats suitable for import into Scoops3D. QGIS facilitates post-simulation analysis as well, with slope stability results capable of being overlaid against other spatial information such as proximity to roads and land use for a comprehensive understanding of risk within the subject area.

3.1.4 Inputs to the Scoops3D software

As already mentioned earlier, Scoops3D is used in this thesis to assess the stability of slopes in specific districts of Rwanda. The software evaluates rotational, spherical slip surfaces that encompass multiple DEM cells. Scoops3D performs a systematic search of the DEM, maintaining a record of the lowest factor of safety for each cell and tracking the most unstable potential failure in the domain, whose results can easily be exported to QGIS for further visualization and analysis[24]. Following are some key dataset inputs in the computational analysis:

- DEM which defines the topographic surface.
- Soil properties : cohesion, angle of internal friction, and unit weight from various literature and Harmonized World Soil Database(HWSD).
- Groundwater configuration parameterized through the pore prossure (or the pore pressure ratio).
- Seismic loading conditions: PGA was obtained from regional earthquake data by ground Motion Prediction Equations (GMPEs) for East Africa[26]. For different magnitudes M:

$$M = 5.0: \quad Y = 1.42 \exp(1.43M)R^{-1.1} \tag{3.12}$$

$$M = 5.5 - 6.5: \quad Y = 1.42 \exp(1.43M)R^{-1.2}, \tag{3.13}$$

  where Y is Peak Ground Acceleration(PGA) and R is the epicentral distance, respectively measured in gal and kilometer (km).

The maximum PGA (see Figure [7]) calculated by using GMPE (equation: 3.12 and 3.13) agrees with the seismic assessment done for the Rubavu region which is near the study area, Karongi district, where it is recommended that the PGA is 1.6 m/s^2 (0.163g)[27]. The results, with the FOS maps coming from Scoops3D, were brought back into QGIS for further processing. Overlays of land use maps and other spatial data have been used to show how factors like economic activities and infrastructure match up with zones of high risk.

3.1.5 Integration of Tools

The workflow depicted in Figure 3 integrates DEM data, QGIS, and Scoops3D. DEM served as the base data, while in QGIS all the operations on data pre-processing, visualization, and exporting the input data for the simulations are done. Scoops3D was generating critical outputs since it performs the slope stability analysis, and its results are again re-processed and visualized in QGIS to get helpful insights about slope stability.

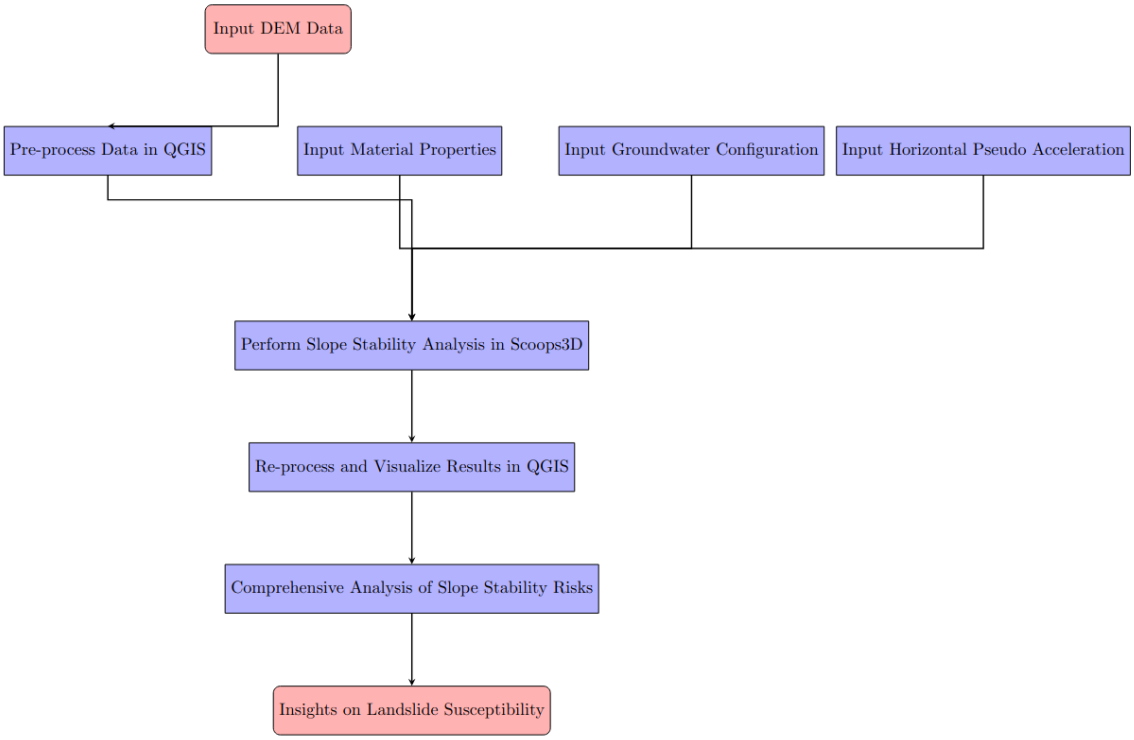

Figure 3: Building analytical model

The set of tools provided the possibility of a comprehensive analysis of slope stability in the Karongi District considering topographic, soil, and land use factors and seismic loading affecting landslide susceptibility.

3.2 Study area: Karongi District

Karongi District 4 is located in the western province, Rwanda, bordered to the west by Lake Kivu. The topography is generally mountainous with steep slopes.

The total area of the district is about 993 square kilometers, at altitudes that vary from approximately 1,460 meters at the shores of Lake Kivu to over 2,000 meters in the highlands [28]. It is a part of the Albertine Rift, which has a rugged topography and largely contributes to its high susceptibility to landslides.

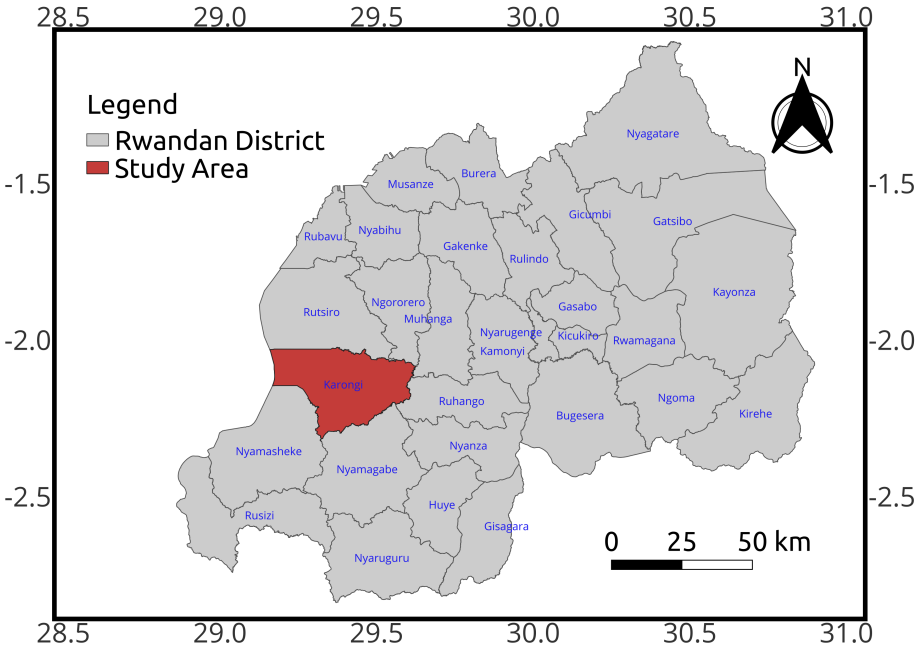

Figure 4: Location of the study area.

Karongi has a tropical highland climate with two major rainy seasons between March and May and from September to November. These contribute to quite frequent landslides. High rainfall combined with steep slopes and variable geology comprising volcanic and metamorphic rocks on the whole contributes to slope instability in Karongi.

The National Institute of Statistics of Rwanda estimates that the district has a population density of 482 inhabitants per square kilometer. The people depend mainly on subsistence farming, while in the district, land use is mostly agricultural. This predisposes them to landslides, along with steep slopes in the region.

Recent studies have identified Karongi as a high-hazard zone for landslides [10]. They indicated geology, rainfall, elevation, seismic loading and proximity to rivers and roads as key factors contributing to the susceptibility to landslides within the area. With these attributes, Karongi is one of the important areas where research on landslide hazard is being considered and, thus, ideally suited for numerical simulation of slope stability problems under different loading con-

ditions.

3.3 Landcover/ Landuse of Karongi District

Land cover/land-use map of Karongi District is mapped in Figure 5, where the spatial distribution of the various land classes, such as forests, rangelands, settlement areas, roads and bare ground, is shown. This map, in a general sense, shows that a large portion of the area is dominated by rangeland soil (orange) and bare soil (light beige). The built-up areas, shown in red, though smaller in spatial extent, are concentrated in a few particular regions, often near transportation corridors and settlements. The water body in the northwest is the district's portion of Lake Kivu-a main geographical feature.

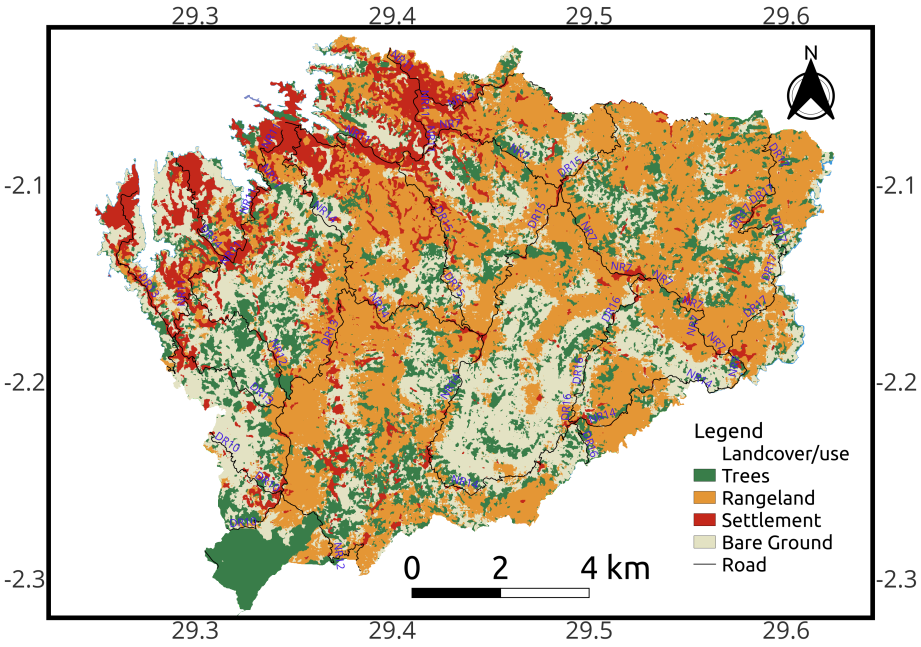

Figure 5: Land Cover and Land Use Map of Karongi District (01/01/2023 - 01/01/2024), downloaded from:https://earthexplorer.usgs.gov/

Each one of these land cover classes may have a different implication for slope stability. For example, the areas covered with forests improve soil stability due to root reinforcement and could thus potentially reduce the risk of a landslide. In contrast, bare grounds and built-up areas might have insufficient vegetation cover or root structure to support the ground or prevent erosion and landslides, especially in steep slope conditions. Distance to roadways increase susceptibility to landslides due to disturbance of soil and changed drainage [11]. This understanding is relevant to the study because the research seeks to discuss the

differences among various types of land use in terms of landslide susceptibility within Karongi District.
These QGIS-processed land use maps present the in-depth context of the slope stability analysis and serve the objective of the study to explore the influence of changes in land use and cover on landslide occurrences in western Rwanda.

3.4 Soil structure and geotechnical parameters.

The study area is made up geologically of a diverse lithology comprising pelitic rocks, Quartz-Phyllites, Granites, Granite-Gneisses, Mica-Schists, Amphibolites, and Meta-Volcanics-manifestations of geological formations. Major class developments of soils in the region are highly influenced by these types of rocks, with the dominant soils formed from altered granite and gneiss. The main dendritic and trellis drainage patterns in the area significantly govern the soil behavior and stability. Metamorphic rocks in general constitute the base geology; tectonic activities during the Pleistocene resulted in breaks in drainage, culminating in the formation of alluvial soils, which are generally more erodible. Such a combination of geological and hydrological factors contributes to the soil properties in the region, including cohesion, shear strength, and permeability, which also become critical in understanding slope stability and landslide risks in the study area [19].

3.5 Input parameters and assumptions.

Slope stability analysis was carried out with Scoops3D using various input parameters and assumptions. These kinds of parameters and assumptions are considered in order to simplify real conditions of the slope and, at the same time, remain as true to the actual performance of the slope under different loading scenarios. Major input parameters and assumptions that were implemented during the analysis are presented below.

3.5.1 Input parameters

- **Soil Properties:** The model requires some soil properties such as cohesion, angle of internal friction, and unit weight. These parameters determine the shear strength and stability of soils in the study area. Wherever possible, these soil properties are deduced from available geotechnical surveys or estimates them from similar soil types in the region. Table 1 shows some of the soil parameters as reported by the Rwanda Ministry of Agriculture and Animal Resources (MINAGRI).

- **Groundwater configuration:** The pore-pressure ratio, r_u, has been selected for the groundwater configuration parameter in Scoops3D for the purpose of this study because specific data could not be available for the other options like piezometric and 3D pressure heads. Thus, the pore-pressure ratio method predicts pore-water pressures as some fraction of

No	Soil property	symbol	Units
1	Cohesion	C	9 kPa
2	Angle of Internal friction	ϕ	25°
3	Unit Weight	γ	19 kN/m^3

Table 1: Recommended soil parameters[29].

the weight of the overlying column and hence provides an effective approximation within the constraints of the available data.
Pore-water pressure is given by the relation of pressure head h as:

$$u = h \cdot \gamma_w \tag{3.14}$$

where u is the pore-water pressure, h is the pressure head and γ_w is the unit weight of water[17, 24].

[17] developed the following equation that defines the pore-water pressure ratio (r_u):

$$r_u = \frac{u}{\int \gamma \, z \, dz} = \frac{u}{W/A_h} \tag{3.15}$$

where:

- γ is the unit weight of the overlying material,
- W the total weight of the soil column,
- A_h the horizontal area.

This pore-water pressure ratio has a great impact on the soil shear strength as previously discussed in section 3.1.1 especially on equation 3.5. For the purpose of this analysis, the following values $r_u = 0$, $r_u = 0.1$, 0.2 and $r_u = 0.3$ were assumed in order to test increasingly high pore pressures and their impact on slope stability.

- **Seismic Coefficients:**

  To assess the stability of a landslide under seismic loading conditions, Scoops3D requires only one horizontal pseudo-acceleration coefficient K_{eq} as a fraction of gravity g. This would give a measure of the seismic load that is subjected to the slope. In the frame of the present study, four important earthquake events affecting Karongi district of Peak Ground Acceleration (PGA) as shown in Figure [7] were selected and presented in table 2.

No	Date	Latitude	Longitude	Magnitude (Mb)
1	2002-10-24T06:08:37.980Z	-1.884	29.004	6.2
2	2008-02-03T07:34:12.180Z	-2.296	28.9	5.9
3	2015-08-07T01:25:02.540Z	-2.1412	28.8973	5.8
4	2003-03-20T06:15:20.580Z	-2.418	29.56	5.2

Table 2: Selected Earthquake data (https://earthquake.usgs.gov/).

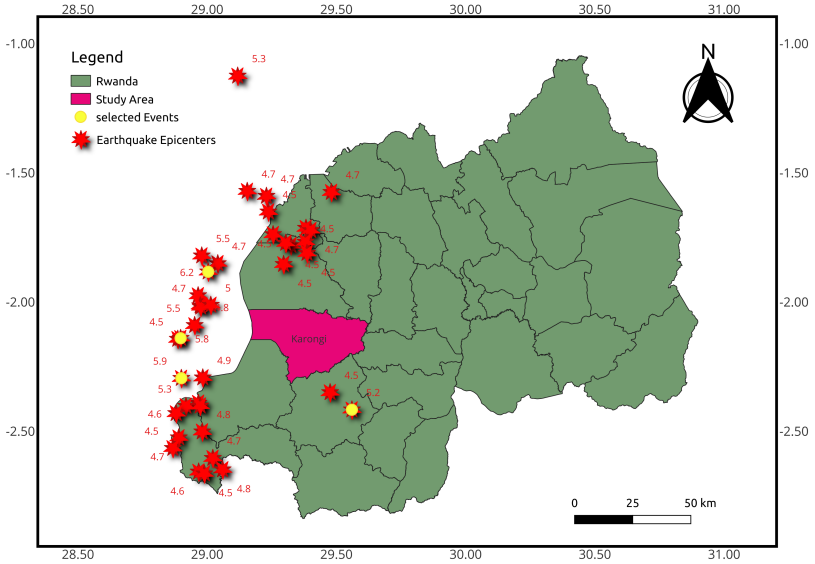

Figure 6: Earthquake locations relative to the study area (https://earthquake.usgs.gov/earthquakes/search/)

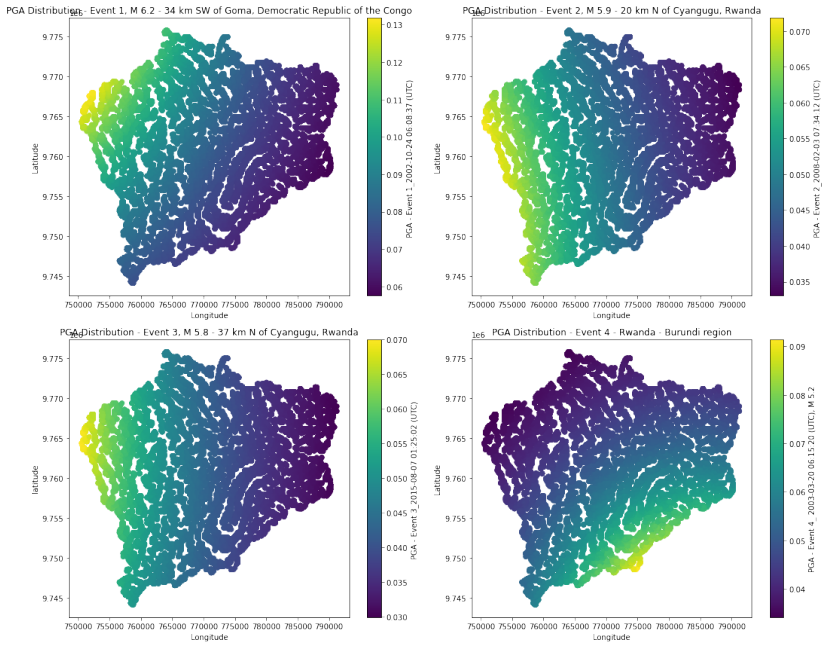

Figure 7: PGA distribution in the study area for the four selected earthquakes.

These four earthquakes have been located in Figure [6], making the spatial distribution more clear regarding seismicity and its relation to the Karongi district. It should be noted that in this study, only the land part of Karongi district is considered, excluding the western part, which is part of Lake Kivu.

Instead of selecting the PGA from a single event, an average PGA of 0.065 g from these four events was selected due to several reasons:

- **Representative Averaging:** The four earthquakes analyzed show different spatial distributions and magnitudes of PGA across the region 7. Thus, averaging the values of PGA yields a K_{eq} of 0.065 g representative of the seismic impact across the four events rather than focusing on a single earthquake. This would ensure that the model captures a general seismic hazard level reflecting the typical PGA expected in the region over time.
- **Consistency with Regional Seismic Hazard:** Regional seismic hazard assessments usually involve averaging the values from multiple significant events to smooth out local variabilities and avoid the over-representation of a unique characteristic belonging to any single event. This provides a balanced view of the seismic hazard considered sound for modeling and planning.

- **Simplified Modeling Requirement:** In this regard, only one value of K_{eq} is needed in Scoops3D for stability calculations. Using the averaged PGA of 0.065 g provides a balancing input that does not complicate the modeling process and hence is sufficiently representative for seismic conditions particular to Karongi district.
- **Relevance of Selected Earthquake Events:** The selected earthquake events are historically very important, with a variety of seismic sources related to Karongi. Averaging the PGA distributions from these events provides an approximation of seismic loading commonly experienced in the region, approximated by the selected K_{eq} value of 0.065.
- **Consideration of Safety and Sensitivity:** Instead of maximum, the use of average PGA will avoid placing too much emphasis on extreme values that may not be representative of regular seismic activity in the area. A sensitivity analysis would further show that the factor of safety in Scoops3D does not change significantly between using the average and using the maximum or minimum PGA values and further validate this approach for hazard assessment.

In this regard, the 0.065 average value of K_{eq}, based on the PGA distribution of these important earthquake events, would correspond to a balanced approach in modeling the stability of landslides under seismic loading and would ensure effective hazard representation by meeting the requirements of the modeling tool itself.

3.5.2 Wrap-up of the basic assumptions

1. **A homogeneous material property** was assumed for the subsurface conditions across the study area and taking uniform values for cohesion, angle of internal friction, and unit weight.

2. **Spherical Slip Surfaces:** Scoops3D assumes potential failure surfaces are spherical in shape, undergoing rotational slip. This assumption simplifies the identification and analysis of potential landslides by the use of fixed geometry, which actually comes in line with common failure mechanisms in natural slopes[24].

3. **Method of Columns:** These 3D method-of-columns approaches divide the failure mass into vertical columns. It is assumed that each column moves as a rigid body internally undeformed, thus providing a simplification in the model due to the fact that each column can be treated independently, which subsequently allows the program to perform the calculation of shear forces at the base of each column[24, 16].

4. **Neglect of Side Forces:** Both the Ordinary method of Fellenius and Bishop's Simplified method assume zero side forces between adjacent columns. Such simplification reduces the computational complexity but at some

expense in accuracy when the lateral interactions between columns are significant.

5. **Rigid Failure Mass:** The failure mass is assumed to be a rigid body, with all columns having uniform movement along the slip surface. There is no consideration for internal progressive failure within the slip surface in this study to maintain consistency in the calculation of FOS.

6. **Pseudo-Static Earthquake Loading:** Seismic forces are modeled by using a simplified pseudo-static approach, whereby each column is subjected to a horizontal force proportional to the seismic coefficient (k_{eq}). This greatly simplifies the process of earthquake loading but it does not take into account the dynamic effects of the ground shaking.

4 Results

This section presents the results of the slope stability analysis for Karongi District through Scoops3D model simulations considering various conditions. The factors of safety maps integrated over different scenarios study the effect of seismic loading represented by an average PGA of 0.065g, groundwater conditions represented by pore water pressure ratio, and soil properties. These are real conditions affecting slope instability in this study area.

4.1 Slope Stability analysis based on seismic loading

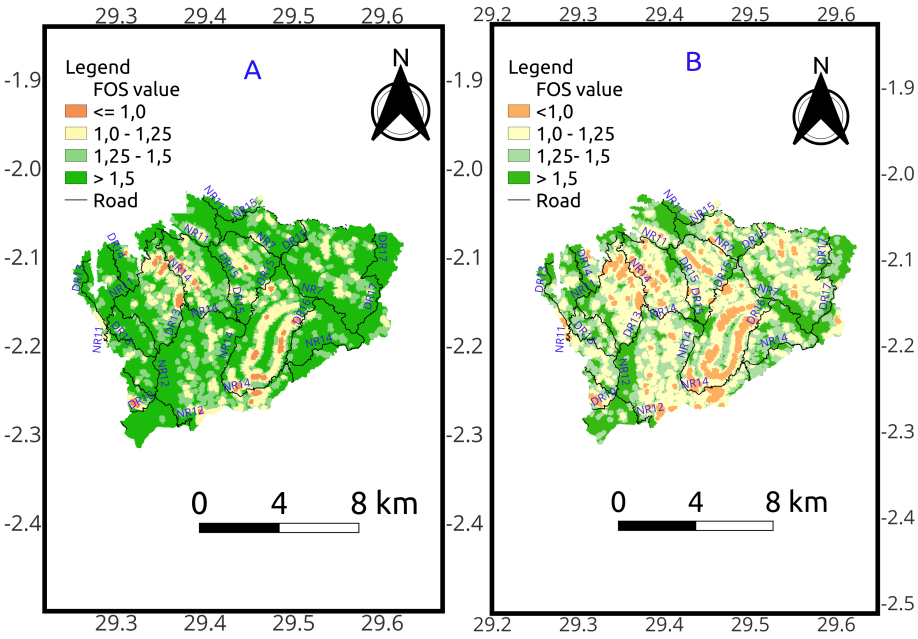

Figure 8: A) The FOS for pore water pressure ratio, $r_u = 0.0$ and horizontal pseudo-acceleration coefficient(fraction of g), $k_{eq} = 0.0$; B) The FOS for pore water pressure ratio, $r_u = 0.0$ and horizontal pseudo-acceleration coefficient(fraction of g), $k_{eq} = 0.065$.

- **Pore Water Pressure Ratio, $r_u = 0.0$ and Horizontal Pseudo-Acceleration Coefficient $K_{eq} = 0.0$**: The map 8.A. reflects the baseline slope stability at static conditions, without seismic force and excess pore water pressure impacts. It represents a control scenario: areas of higher and lower stability result purely from topographic and geotechnical properties in this analysis. These results outline the base level of understanding for stability before dynamic considerations are applied.

- r_u **= 0.0 and** K_{eq} **= 0.065:** This analysis incorporates the effect of seismic forces ($K_{eq} = 0.065$) under dry conditions ($r_u = 0.0$) 8.B). The results show a remarkable reduction in slope stability compared to the static case, with larger areas moving into possible instability. This indicates the important role of seismic loading in slope failures.

4.2 Slope stability analysis based on pore water pressure ratio

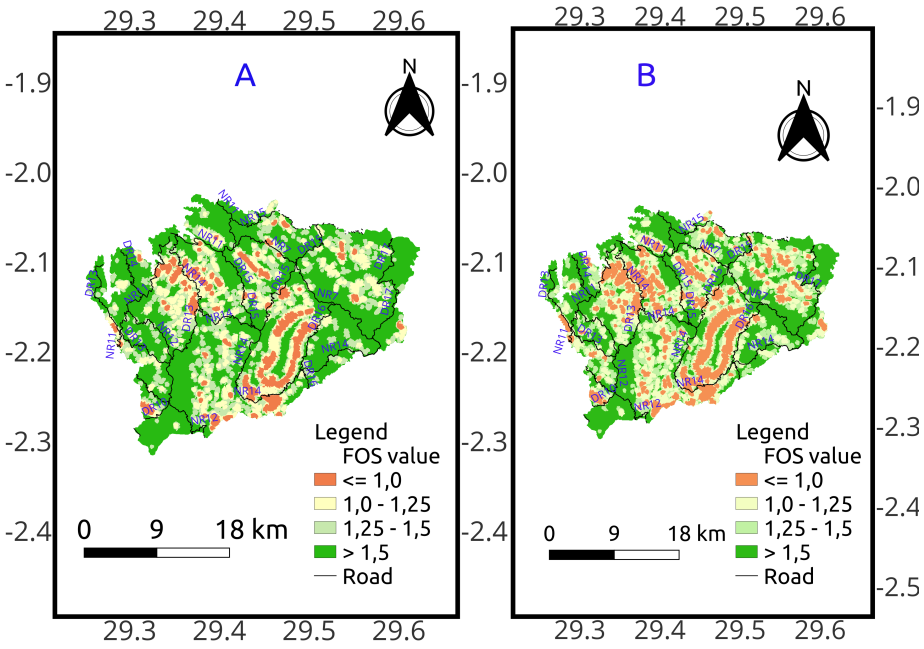

Figure 9: A: The FOS for pore water pressure ratio, $r_u = 0.1$ and horizontal pseudo-acceleration coefficient(fraction of g), $k_{eq} = 0.0$, B: The FOS for pore pressure ratio, $r_u = 0.2$ and horizontal pseudo-acceleration coefficient(fraction of g), $k_{eq} = 0.0$

Progressive increase of pore water pressure ratio to medium magnitude r_u =0.1 (Figure 9.A), without seismic forces represents areas in low lying areas and in the concave element of slopes and demonstrates extensive increase in unstable areas where the pore pressure is obviously elevated due to water infiltrations thus decreasing the shear strength that implies less slope stability. For higher pore-pressure ratios ($r_u = 0.2$), this map (Figure 9.B) shows a significant increase in unstable zones. From this, it can be developed that long or heavy rainfall events resulting in increased pore pressure have a great influence on slope stability, even without seismic activities.

4.3 Slope stability analysis for combined pore water pressure ratio and seismic loading

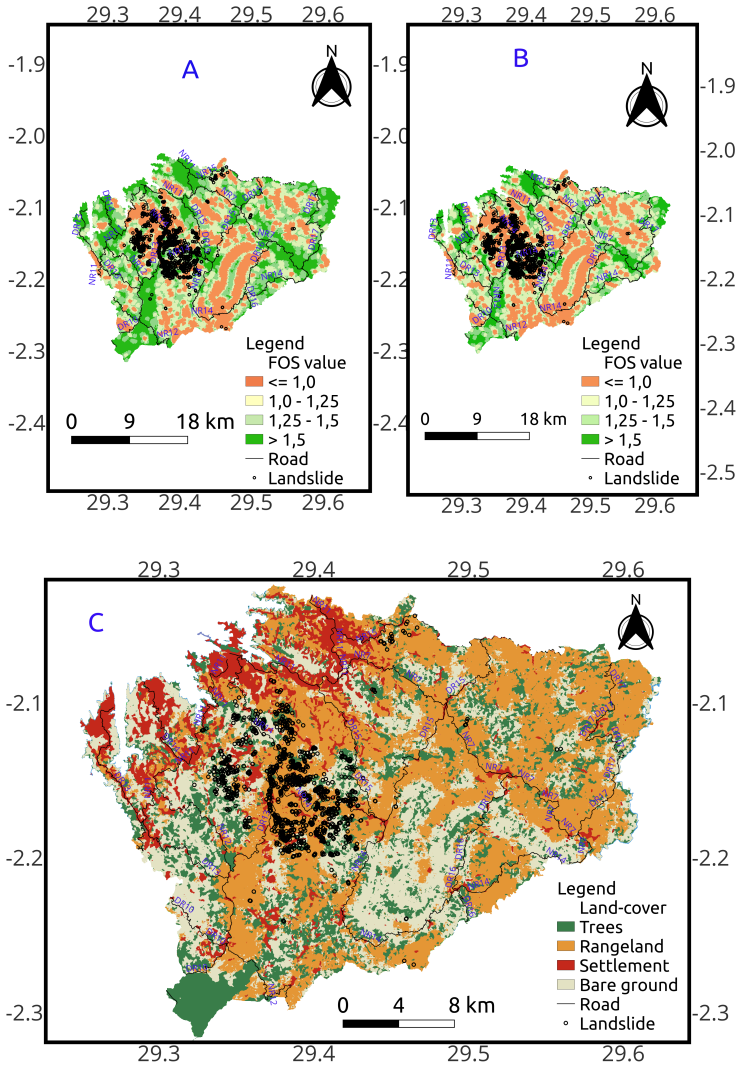

Figure 10: A)The FOS for pore water pressure ratio, $r_u = 0.1$ and horizontal pseudo-acceleration coefficient(fraction of g), $k_{eq} = 0.065$. B)The FOS for pore water pressure ratio, $r_u = 0.2$ and horizontal pseudo-acceleration coefficient(fraction of g), $k_{eq} = 0.065$. C) Land cover/use with historical landslides of the study area. [Shallow landslide inventory for 2000-2019 (eastern DRC, Rwanda, Burundi) : https://zenodo.org/records/5027004[30]]

Historical landslide overlay over this map (Figure 10 .A), in fact validates the analysis as considerable alignment of the predicted unstable zones and the past events of landslide. It would seem that moderate pore pressure in conjunction with seismic forces have combined to provide quite a realistic scenario of natural slope instabilities.

At the most extreme conditions examined here, namely high pore pressure with seismic influence, the map (Figure 10 . B) suggests a very large area is unstable, with particularly severe effects in the landslide prone areas. This tends to validate our hypothesis that such conditions constitute critical thresholds for slope failure within the study area. Slope stability analysis for Karongi District provides a picture of the multifaceted interaction between natural and anthropogenic causes that modulate landslide susceptibility. From this analysis, the outputs show how, in relation to slope stability in the Karongi District, the integrated effects of soil properties, slope gradients, groundwater conditions, seismic loading, and land use come into play, hence highlighting areas that could be in need of mitigation measures.

5 Discussion and Conclusion

The objective of this section is to review the most important results obtained from the numerical simulations, as done in Scoops3D in order to investigate scenarios of slope stability by varying loading conditions of Karongi District. The maps of FOS obtained in this work provide the variation of slope stability in scenarios considering different pore pressure ratios, DEM, soil properties and seismic loading. Such results will be critically interpreted in order to have useful insights about susceptibility to landslide in the investigated area.

5.1 Comparative Analysis of Factor of Safety Maps:

The presented FOS maps show in detail the variation in stability of slopes for different pore water pressure ratios, $r_u = 0.0$, 0.1, and 0.2, and seismic loading conditions, $k_{eq} = 0.0$ and $k_{eq} = 0.065$ g. With the classification of FOS values regarding stability classes, as represented in Table 3, the analysis puts into unstable, quasi-stable, moderately stable, and stable areas in the study region.

Table 3: Classification of factor of safety [31]

Factor of Safety (FOS)	Slope State	Remark
< 1.0	Unstable	Stabilizing factors are needed for stability
$1.0 - 1.25$	Quasi-stable	Minor destabilizing factors lead to instability
$1.25 - 1.5$	Moderately stable	Moderate destabilizing factors lead to instability
> 1.5	Stable	Only major destabilizing factors lead to instability

This classification will serve to outline how different factors influence slope stability.

Unstable Slopes (FOS $<$ 1.0):

With r_u= 0.0 and k_{eq} = 0.0, there is no pore pressure and seismic loading, but FOS in some parts is already below 1.0, hence unstable (Figure 8.A). Based on the given classification, it is said that these slopes should undergo additional stabilizing measures since there is a possibility of landslide occurrence in such areas [31]. That would mean topographic and geotechnical conditions alone in these areas are enough to trigger an instability portrayed by the Scoops3D model based on DEM and soil properties. The larger the pore pressure, the more areas fall into this unstable category. This implies that higher infiltration of groundwater likely resulting from intensive rainfall-markedly raises the susceptibility to landslides of areas already vulnerable.

Quasi-Stable Slopes (FOS 1.0–1.25):

Areas classified as quasi-stable-that is, with FOS between 1.0 and 1.25-show small stability that can easily be destroyed by relatively small external forces such as minor seismic activity or fluctuations in pore pressure.
These slopes are prone to instability because of the prevalence of small perturbation factors, especially when pore pressure ratios lie between 0.1 and 0.2 (Figure: 9). In practical applications, quasi-stable areas may require monitoring since they are at the threshold of instability and could easily switch to unstable with slight changes in environmental conditions.

Moderately Stable Slopes (FOS 1.25–1.5):

It was considered that the slopes with a FOS ranging from 1.25 to 1.5, although moderately stable slopes, still be resistant but could fail due to more moderate influences of destabilization factors, such as higher pore pressures and seismic events. These areas usually correspond to slopes where r_u values increase up to

approximately 0.2 in this study (Figure 10.B).
This means that, though these slopes are currently stable, they would be prone to moderate changes in hydrological or seismic conditions and, therefore, may require mitigation efforts to remain stable under extreme events.

Stable Slopes (FOS $>$ 1.5):

The slopes with FOS values above 1.5 can be considered as stable, where only the occurrence of sufficient destabilizing factors-higher pore pressure and seismic loading-could provoke failure [31]. In general, such areas usually represent the slopes that have inherent stability because of favorable topographic and geotechnical conditions, which in fact were reflected in the DEM analysis in Scoops3D. The more stable slopes would be less likely to need immediate interventions; however, they could form part of broader strategies related to risk management in view of probable environmental changes.

In other words, this classification system illustrates how the interrelation between the pore pressure and seismic loading bears on slope stability. It contains quasi-stable and moderately stable zones where even slight changes in the environment may seriously alter the conditions of stability; hence, the need for early warning and mitigation in those areas [31],[30].

5.2 Seismic Influence on Slope Stability

Seismic forces marked with noticeable impacts on slope stability in Karongi District. The decision to use an average seismic coefficient, $k_{eq} = 0.065$ g, deduced from PGA values of historical earthquake events (Figure:7), therefore allows seismic loading to be estimated in a realistic yet conservative way. This averaged coefficient accounts for seismic variability without overstating risk and hence provides a balancing input in general seismic hazard assessment.

The FOS maps both with and without seismic loading indicate that even moderate seismic forces ($k_{eq} = 0.065$ g) greatly reduce stability in steep areas. A comparison of the maps for $k_{eq} = 0.065$ g with those for $k_{eq} = 0.0$ g shows a clear reduction in FOS values with seismic loading amplification (Figure 8). These results really bring out the importance of seismic resilience, suggesting that areas of higher seismic forces may benefit from targeted slope reinforcement and drainage management to mitigate landslide risk [30].

5.3 Impact of Land Use on Susceptibility to Landslide

Land use is quite an influencing factor in slope stability in the Karongi District, which could be obtained from the overlay presentation of land use classes and historical landslides locations maps (Figure 10.C). Generally, land uses, like bare soil or agricultural(rangeland), settlement, proximity to roads tend to have high concentration of landslides and are hence prone to landslides, particularly

in steep slope areas [32].

In this respect, the correlation of land use and stability strengthens the call for land management strategies that involve vegetation cover into high-risk areas. The overlays further show the areas of proximity to infrastructure such as roads where meta-stability can be reduced by disturbance of the soil and alteration of drainage[32], [10]. These findings therefore denote proximity to infrastructure as an exacerbating factor towards slope instability, hence the call for careful planning and construction practices in order to prevent the occurrence of landslides.

5.4 Landslide susceptibility analysis and its validation using historical data

5.4.1 Historical landslide data validation.

Figure 10.A and B present the overlay of historical landslide locations [Shallow landslide inventory for 2000-2019 (Karongi) : https://zenodo.org/records/5027004][30] on a FOS map for $r_u = 0.1$ with $k_{eq} = 0.065$, and a FOS map for $r_u = 0.2$ with $k_{eq} = 0.065$ respectively, which itself is a very useful validation of model predictive capability. Historical landslide events align well with those areas having low FOS values (FOS <1.0), proving that the model can reliably identify the zones of high susceptibility. This agreement speaks well for the model's accuracy in correctly predicting the landslide risks in the Karongi region and lends confidence in its applicability to similar slope stability assessments in Western Rwanda.

Where modeled instability and historical landslides are in disagreement, such discrepancies may be due to factors not modeled, such as critical soil heterogeneity or local hydrological conditions. Overall, the good correlation observed makes it possible to consider the model a useful tool for landslide risk assessment and early warning in Karongi and similar highland areas.

5.4.2 Landslide Susceptibility predicted in the eastern part of the study area

While the model validation against historical landslides data enhances its credibility, it also indicates low values of FOS in areas where no historical landslides have been recorded. One such zone is found in the Southeast part of the Karongi District and exhibits a peculiar "horseshoe" shape with low FOS values (See figure 10 A and B). Such areas are envisioned to have a high susceptibility to landslide, especially under high pore water pressure ratio likely caused by the extreme rainfall events, despite present-time zero or very low records of landslide occurrences. The landslides susceptibility of the eastern region of Karongi district can be attributed to its nature.

Land-use data in the study area, as illustrated on the figure 10.C, shows that the area is basically characterized by bare ground with little or no vegetation cover. The absence of forested areas or significant vegetation cover reduces the root reinforcement effect, an important factor in slope stability [11]. This makes the area very prone to soil erosion and slope failure during intense rainfall. It will also be necessary to undertake in-depth investigation of the groundwater configuration and geotechnical parameters of the soil of this area with "horse-shoe" shape of eastern part of Karongi district, like cohesion, angle of internal friction, and unit weight, to check whether they are significantly different from the rest of the study area. While this is the case, the eastern part of the study area provides a special case, which is expected to be prone to landslides in areas where no historical landslides occurred. This again underscores the importance of using predictive models for identifying latent risks that are not immediately obvious from historical landslides data alone. Proactive measures within such areas can go a long way in reducing the potential of landslide events in the future.

5.4.3 Implications for landslide mitigation and prevention

Integrated findings between verified and predicted landslide-prone areas call for a joint effort for the management of landslide hazards; therefore, for the northwest part of Karongi District, reinforcements of already known prone to landslides areas have to be carried out by taking an advantage of the good consistency of historical data and predictions made by the model, the required measures would include slope stabilization by putting in place appropriate drainages to control the movement of water during rainfall coupled with community awareness.
While this is the case, the predicted susceptibility of the eastern part, with very low historical landslides, makes it quite a unique challenge. It signifies the essence of predictive models in pinning latent risks that could hardly be obtained from historical records only. Proactive measures can reduce the potential for such cases of landslide events. This includes detailed geotechnical investigations, land-use planning that discourages development in high-risk zones, and measures to increase vegetation cover for natural slope reinforcement.

The model's capability for showing coherence with the historical landslide pattern, as well as the identification of new susceptible areas, justifies it as an effective tool for landslide risk assessment. Historical data on landslide incidents in the northwestern part of Karongi District have validated the model's prediction, hence reliable for guiding mitigation efforts in this high-risk region. At the same time, the model predictions of low FOS in the eastern region call for pre-emptive actions to address potential landslide risks in areas with no previous incidence. The present findings highlight the necessity to incorporate predictive modeling along with on-ground mitigation strategies in developing landslide hazard resilience across the study area.

5.5 Sensitivity to model assumptions

The model is based on a number of assumptions that, while simplifying the data input, most probably at the cost of precision, carry several implications for the computation and interpretation of the FOS (See section:3.5.2). First, the homogeneous soil property assumption assigns uniform values for cohesion, angle of internal friction, and unit weight to the soil. Future investigations may take into consideration spatially variable soil parameters for capturing fully the impact of heterogeneity on the stability of the slopes.

Besides, the assumption of spherical slip surfaces matches many natural landslide scenarios but in some terrains may not represent complex failure surfaces. Being able to recognize such limitations becomes an important step toward refining assessments in landslide risk, where alternative geometries of slip surfaces might permit an improved understanding of local instability.

This is simplified from the inherently dynamic nature of seismic loading, which in this approach is represented by static horizontal forces being proportional to the seismic coefficient. While the method is computationally efficient, it fails to capture the temporal aspect of seismic ground motion. For better representation of earthquake effects-especially those events with high magnitudes-future studies could be directed to dynamic seismic loading.

The discussion on slope stability results in Karongi District shows a high impact that is influenced by pore pressure, seismic loading, and land use. These findings show the role of pore pressure and seismic events in destabilizing slopes and that forest cover reinforces slope stability. The model is also partly validated by historical data on landslides, hence useful in landslide susceptibility analysis within Karongi district, Western Rwanda. Whereas there are simplifications concerning the properties of soils, slip surfaces, and seismic modeling, the assumptions provide avenues by which future research could refine the model as it aims at improving predictability.

5.6 Conclusion

This thesis presented a numerical simulation of slope stability and landslide susceptibility in the Karongi District under various loading conditions. Some of the key findings from this study are:
Pore water pressure ratios and slope stability: The study revealed that increasing pore water pressure ratio greatly decreases slope stability, with FOS values falling below 1.0 in areas of critical safety. This points out the susceptibility of the area to landslides due to heavy rainfall and groundwater infiltration since the pore water pressure ratio is most likely increased by intense rainfall in the Karongi district.

Seismic influence: The incorporation of seismic loading, represented by an

average Peak Ground Acceleration of 0.065g, showed that moderate earthquakes have increased slope instability, especially in those already classified as quasi-stable or unstable areas.

Land use and cover: The proximity to roads, settlement, bare and agricultural lands are more susceptible to landslides.

Landslide susceptibility and validation with historical data: The modeled unstable zone alignment with historical landslide locations in the North-West part of the study area and the other few regions of the Eastern part, validated the reliability of the Scoops3D simulations, further strengthening the applicability of the approach in this work as being suitable for risk assessment. At the same time, the model predictions of low FOS regions in the eastern part of the study area call for proactive actions to address potential landslide risks in areas with no previous incidence. The present findings highlight the necessity to incorporate predictive modeling along with on-ground mitigation strategies in developing landslide hazard resilience across the study area.

This research study provides actionable insight into the interplay of topographic, geotechnical, seismic, and environmental variables that influence slope stability in the Karongi District. It further helps in the integration of geospatial tools, numerical modeling, and comprehensive datasets that are effective for landslides risk management. Further refinement of soil property data, groundwater configuration in the relationship with rainfall and incorporation of dynamic seismic loading are recommended for future research to enhance predictive accuracy. By addressing these areas, this research lays the groundwork for informed decision-making and proactive mitigation strategies to reduce landslide risks in Rwanda and similar regions globally.

Appendix A: Collected data

The following is a list of all the data collected for this study.

1. Topographic data(DEM) of 10m resolution with a size of 287,1MB
2. Harmonized World Soil data (HWSD) with a size of 91,6MB
3. Harmonized World Soil Data Raster with a size of 1,9GB.
4. Landuse and Land Cover data for Rwanda from 01/01/2023 to 01/01/2024 (downloaded from:https://earthexplorer.usgs.gov/) with space of 368,1MB
5. Earthquake catalog data for Rwanda (From 2002 up to 2023) downloaded from USGS with size of 62,6kB.(https://earthquake.usgs.gov/earthquakes/search/)
6. Administrative Boundaries Data(Shapefiles) with size of 2,9MB.
7. Shallow landslide inventory for 2000-2019 (eastern DRC, Rwanda, Burundi) : https://zenodo.org/records/5027004[30]

Appendix B: Python code used to plot the Peak Ground Acceleration (PGA) distribution within the study area

In [12]:

```
import pandas as pd
import matplotlib.pyplot as plt

# Load the Excel file
file_path = '/home/sylvain/Documents/Slope_stability_and_landslides/Exercise1/Four_PGA_New_Par.xlsx'
data = pd.read_excel(file_path)

# The Excel file contains four separate PGA columns for each event
x = data['Longitude']
y = data['Latitude']
pga_event1 = data['PGA_Event1']  #  Event 1
pga_event2 = data['PGA_Event2']  #  Event 2
pga_event3 = data['PGA_Event3']  #  Event 3
pga_event4 = data['PGA_Event4']  #  Event 4
pga_event5 = data['PGA_Event5']  # Event 5

# Set up a figure with 4 subplots
fig, axes = plt.subplots(2, 2, figsize=(15, 12))

# Event 1
scatter1 = axes[0, 0].scatter(x, y, c=pga_event1, cmap='viridis', marker='o')
cbar1 = plt.colorbar(scatter1, ax=axes[0, 0])
cbar1.set_label('PGA - Event 1_2002-10-24 06:08:37 (UTC) ')
axes[0, 0].set_title('PGA Distribution - Event 1, M 6.2 - 34 km SW of Goma, Democratic Republic of the Congo')
axes[0, 0].set_xlabel('Longitude')
axes[0, 0].set_ylabel('Latitude')

# Event 2
scatter2 = axes[0, 1].scatter(x, y, c=pga_event2, cmap='viridis', marker='o')
cbar2 = plt.colorbar(scatter2, ax=axes[0, 1])
cbar2.set_label('PGA - Event 2_2008-02-03 07:34:12 (UTC) ')
axes[0, 1].set_title('PGA Distribution - Event 2, M 5.9 - 20 km N of Cyangugu, Rwanda')
axes[0, 1].set_xlabel('Longitude')
axes[0, 1].set_ylabel('Latitude')

# Event 3
scatter3 = axes[1, 0].scatter(x, y, c=pga_event3, cmap='viridis', marker='o')
cbar3 = plt.colorbar(scatter3, ax=axes[1, 0])
cbar3.set_label('PGA - Event 3_2015-08-07 01:25:02 (UTC) ')
axes[1, 0].set_title('PGA Distribution - Event 3, M 5.8 - 37 km N of Cyangugu, Rwanda')
axes[1, 0].set_xlabel('Longitude')
axes[1, 0].set_ylabel('latitude')

# Event 4
#scatter4 = axes[1, 1].scatter(x, y, c=pga_event4, cmap='viridis', marker='o')
#cbar4 = plt.colorbar(scatter4, ax=axes[1, 1])
#cbar4.set_label('PGA - Event 4')
#axes[1, 1].set_title('PGA Distribution - Event 4, M 5.0 - 37 km W of Kibuye, Rwanda')
#axes[1, 1].set_xlabel('Longitude')
#axes[1, 1].set_ylabel('Latitude')

#Event 5
scatter5 = axes[1, 1].scatter(x, y, c=pga_event5, cmap='viridis', marker='o')
cbar5 = plt.colorbar(scatter5, ax=axes[1, 1])
cbar5.set_label('PGA - Event 4_ 2003-03-20 06:15:20 (UTC), M 5.2')
axes[1, 1].set_title('PGA Distribution - Event 4 - Rwanda - Burundi region')
axes[1, 1].set_xlabel('Longitude')
axes[1, 1].set_ylabel('Latitude')

# Adjust layout
plt.tight_layout()

# Show the plot
plt.show()
```

Appendix C: Screenshot showing examples of Scoops3D run from command line input.

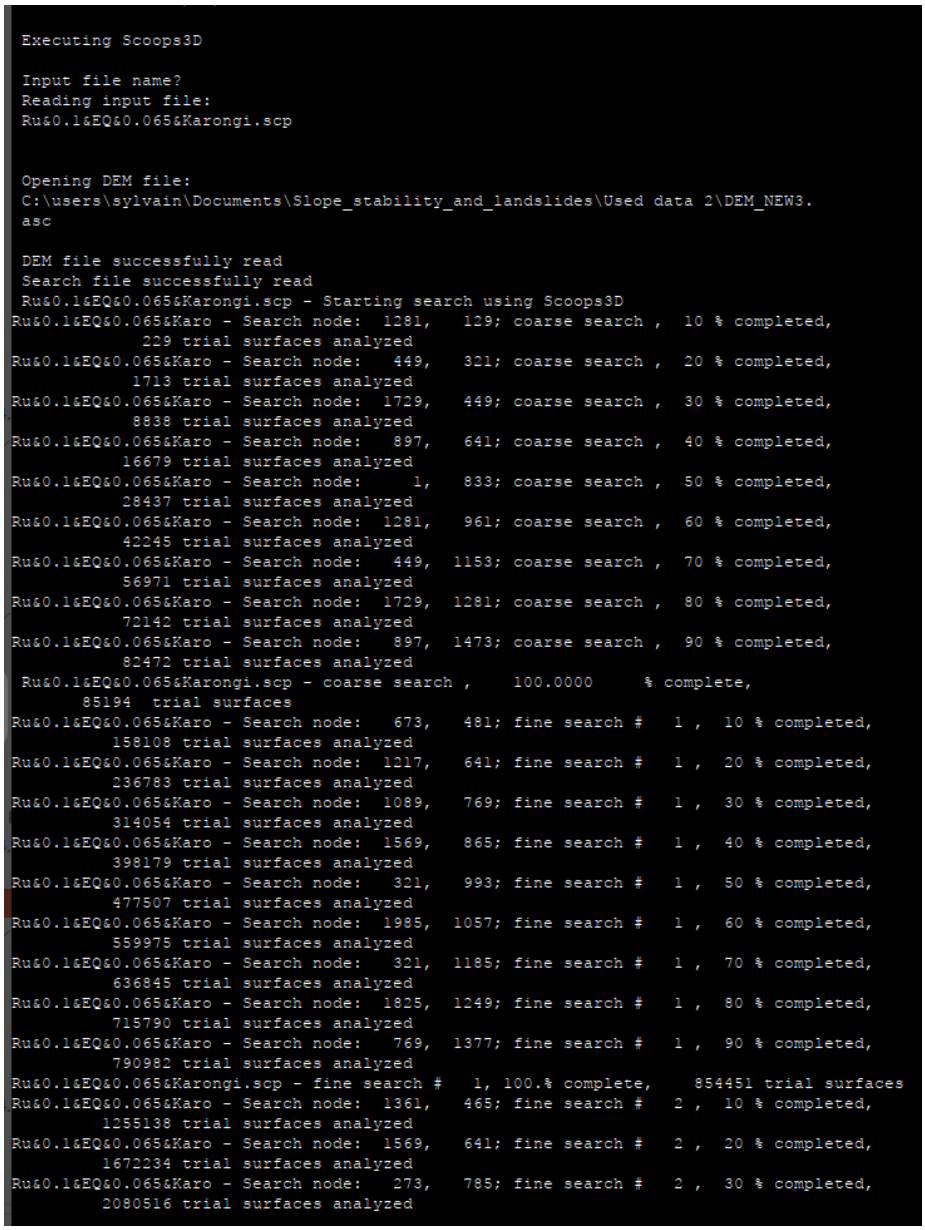

Appendix D: Screenshot of an example of Scoops3D main output file that summarize output files, displaying input parameters and the overall minimum Factor of Safety (FOS).

```
    ************************************************************
                              Scoops3D
          3D Slope Stability Throughout a Digital Landscape
                        U.S. Geological Survey
                             Version: 1.3.01, rev. 03/1/2023
    ************************************************************


This file: C:\users\sylvain\Documents\Slope_stability_and_landslides\Results
New\Ru&0.1&EQ&0.065&December_output\Ru&0.1&EQ&0.065&December_out.txt

Start date and time: 12/20/2024  12:30:21
Description: Ru&0.1&EQ&0.065&December

+++++++++++++++++++++++++++++++++++++++++++++++++++++++++++++++++++++++++++++++
I. INPUT FILES:
  DEM file: C:\users\sylvain\Documents\Slope_stability_and_landslides\Used data
2\DEM_NEW3.asc
  Main parameter input file:
Ru&0.1&EQ&0.065&December.scp

+++++++++++++++++++++++++++++++++++++++++++++++++++++++++++++++++++++++++++++++
II. SIMULATION PARAMETERS:
------------
DEM
Input file for topography: C:\users\sylvain\Documents\Slope_stability_and_landslides\Used data
2\DEM_NEW3.asc
  Dimensions of DEM grid (x,y):                                    2090  1662
  Number of cells in DEM grid:                                      3473580
  Number of non-null cells in DEM grid:                             1975728
  Horizontal resolution of DEM grid (m ):                             19.99
  Minimum elevation of DEM (m ):                                    1460.000
  Maximum elevation of DEM (m ):                                    2582.000
  xllcorner and yllcorner (m ):                      750160.133    9742874.995
------------
UNIT DESCRIPTORS (used for labels in output files)
lengthunits   ceeunits    gammaunits
     m          kPa         kN/m^3
------------
MATERIAL PROPERTIES
Property input method:                                                 layers
Number of layers (nmat):                                                    1
                      total unit wt.
lnum    cee     phi      gamt      ru
        kPa             kN/m^3
  1      9.00  25.000   19.000    0.100
------------
GROUNDWATER CONFIGURATION
Groundwater method (water):                                              Ru
  See material properties for Ru values in each material
------------
EARTHQUAKE LOADING
```

```
EARTHQUAKE LOADING
Horizontal pseudo-acceleration coefficient (dimensionless)(eqcoef):      0.065
------------
LIMIT-EQUILIBRIUM METHOD
Analysis method (method):                                              Bishop
------------
SEARCH METHOD (srch)                                                      box
POTENTIAL FAILURE SIZE CONTROLS
Primary constraint, volume,area,depth (vacriterion):                   Volume
Surface area is not a criterion for size restriction.
Volume range of potential failures (m ^3)(vmin, vmax):    1.000E+07 1.000E+08
Tolerance amount for initial potential failure volume (tol):         1.000E+06
Minimum number of active columns in potential failure required,
      otherwise error message generated (limcol):                        100
SEARCH-LATTICE EXTENT AND RESOLUTION
VERTICAL EXTENT AND RESOLUTION
Minimum elevation of search-lattice nodes (m ) (zsmin):               1500.000
Maximum elevation of search-lattice nodes (m ) (zsmax):               3000.000
Search-lattice vertical spacing (m ) (zsrchres):                        10.000
Increment amount for potential failure surface sphere radius(m )(dr):   10.000
HORIZONTAL EXTENT AND RESOLUTION
Starting search-lattice horizontal node (ismin,jsmin):                    1    1
Ending search-lattice horizontal node (ismax,jsmax):                   2090 1662
Horizontal spacing - multiple of DEM resolution (nsrchres):                8
COARSE-TO-FINE SEARCH PARAMETERS
Horizontal and vertical multiplier for initial coarse search (multres):      8
Search iteration tolerance - percent change F (fostol):                 0.0100
------------
ADDITIONAL OUTPUT FILES AND PARAMETERS
isqout (search quality files):                                             1
irelfos (relative F file):                                                 1
icritlattice (all 3D search centers with FOS for critical centers):        1
isubsurf (3D subsurface factor of safety):                                 3
zfrac:                                                                 1.000
Create new DEM file (remove):                                              A
   (all surfaces with F<foscut removed)
F cutoff for removing material from new DEM (foscut):                1.000E+01

++++++++++++++++++++++++++++++++++++++++++++++++++++++++++++++++++++++++++++++++
III. OUTPUT FILES GENERATED:

     LOCATION FOR OUTPUT FILES:
          C:\users\sylvain\Documents\Slope_stability_and_landslides\Results
New\Ru&0.1&EQ&0.065&December_output\

```

```
      Ru&0.1&EQ&0.065&December_out.txt
      Ru&0.1&EQ&0.065&December_errors_out.txt
      Ru&0.1&EQ&0.065&December_slope_out.asc
        Range: [    0.0000,       62.0318]
      Ru&0.1&EQ&0.065&December_fos3d_out.asc
        Range: [    0.5548,        8.7399]
      Ru&0.1&EQ&0.065&December_ordfos3d_out.asc
        Range: [    0.5117,        6.4658]
      Ru&0.1&EQ&0.065&December_fosvol_out.asc
        Range: [  1.0000E+07,  1.0000E+08]
      Ru&0.1&EQ&0.065&December_spheres_out.okc

     Optional files generated:
      Ru&0.1&EQ&0.065&December_fos3drel_out.asc
        Range: [    1.0000,       15.7526]
      Ru&0.1&EQ&0.065&December_newDEM_out.asc
        Range: [  1271.3646,  2576.7083]
      Ru&0.1&EQ&0.065&December_numcols_out.asc
        Range: [     369,    4020]
      Ru&0.1&EQ&0.065&December_critcheck_out.asc
      Ru&0.1&EQ&0.065&December_boundcheck_out.asc
      Ru&0.1&EQ&0.065&December_subsurffos_out.3D
      Ru&0.1&EQ&0.065&December_critfoslattice_out.3D
      Ru&0.1&EQ&0.065&December_searchgrid_out.asc

++++++++++++++++++++++++++++++++++++++++++++++++++++++++++++++++++++++++++++++++
IV. RESULTS:
Number of trial surfaces tried:                                    21280479
F < foscut found and newDEM_out file created?                           yes
------------
3D POTENTIAL FAILURE - GLOBAL MINIMUM
Bishop's 3D factor of safety:                                        0.5548
Ordinary 3D factor of safety:                                        0.5133
Volume (m ^3):                                                   1.05255E+07
Horizontal surface area (m ^2):                                  2.06499E+05
Slip surface area (m ^2):                                        2.68999E+05
Weight (kg):                                                     1.99985E+08
Number of active columns:                                               572
      x-center         y-center         z-center      radius
     763606.5940     9762559.8142        2830.0000  5.93854E+02
Slip direction, relative to search lattice:                          161.8169
End date and time: 12/20/2024  14:58:01
Elapsed cpu time in seconds:   8.84709E+03
Elapsed cpu time in hours:   2.45753E+00
```

Appendix E: The creenshot of an example of output file contains the minimum 3D factor of safety calculated on the critical surface for each DEM cell

```
ncols          2090
nrows          1662
xllcorner    750160.132699999958
yllcorner    9742874.994659297168
cellsize        19.9947
NODATA_value   9999.0000
1.2629    1.2629    1.2398    1.2011    1.1902    1.1902    1.1769    1.1769    1.1680    1.1611    1.1577    1.1534    1.1
 1.0952    1.0952    1.0952    1.0837    1.0837    1.0837    1.0837    1.0837    1.0837    1.0837    1.0837    1.0837    1.0
 1.0755    1.0755    1.0755    1.0755    1.0755    1.0755    1.0755    1.0755    1.0755    1.0755    1.0755    1.0755    1.0
 0.9541    0.9541    0.9541    0.9541    0.9541    0.9541    0.9541    0.9541    0.9541    0.9541    0.9541    0.9541    0.9
 0.9541    0.9541    0.9541    0.9541    0.9541    0.9541    0.9541    0.9359    0.9359    0.9359    0.9359    0.9145    0.9
 0.9145    0.9145    0.9145    0.9145    0.9145    0.9145    0.9145    0.9145    0.9145    0.9145    0.9145    0.9145    0.9
 0.9359    0.9359    0.9359    0.9359    0.9359    0.9857    0.9857    0.9857    1.0124    1.0597    1.0983    1.0998    1.1
 1.1143    1.1156    1.1172    1.1207    1.1287    1.1310    1.1215    1.1150    1.1136    1.1058    1.0983    1.0955    1.0
 1.0939    1.0939    1.0939    1.1023    1.1136    1.1310    1.1534    1.1528    1.1458    1.1458    1.1458    1.1528    1.1
 1.3376    1.3464    1.3632    1.3587    1.3469    1.3347    1.3347    1.3347    1.3347    1.3760    1.3760    1.4174    1.4
 1.5484    1.5484    1.5714    1.5797    1.6240    1.6892    1.6892    1.6892    1.6892    1.6892    1.6966    1.7057    1.7
 1.8931    2.0189    2.2561    2.2561    2.2561    2.2561    2.2561    2.2561    2.2561    2.2604    2.2604    2.2604    2.4230    2.4
 2.4826    2.4826    2.4609    2.4609    2.4609    2.4609    2.3378    2.3378    2.3378    2.4203    2.4203    2.4203    2.4
 2.5958    2.5958    2.5958    2.5958    2.6368    2.6368    2.6368    2.6368    2.6368    2.6368    2.6368    2.6368    2.6
 2.8298    2.8298    2.8745    2.8745    2.8745    2.8745    2.9273    2.8434    2.8431    2.7365    2.7365    2.7365    2.6
 2.6452    2.6452    2.6452    2.6452    2.6452    2.6452    2.6452    2.5692    2.5480    2.5480    2.5480    2.5480    2.5
 2.1636    2.1636    2.1636    2.1636    2.1636    2.1636    2.1636    2.1636    2.1636    2.1636    2.1636    2.1636    2.1
 2.1636    2.1636    2.1636    2.1636    2.1636    2.1636    2.0742    2.0742    2.0007    1.9918    1.9183    1.9002    1.8
 1.4994    1.4610    1.4610    1.4610    1.4610    1.4610    1.4610    1.4610    1.4610    1.4610    1.4783    1.4746    1.4
 1.3712    1.3652    1.3652    1.3652    1.3652    1.3652    1.3652    1.3543    1.3543    1.3543    1.3543    1.3543    1.3
 1.3543    1.3543    1.3543    1.3543    1.3543    1.3543    1.3543    1.3543    1.3543    1.3543    1.3543    1.3543    1.3
 1.4323    1.4737    1.4737    1.4737    1.4737    1.4898    1.5042    1.4139    1.4021    1.3458    1.3304    1.3304    1.3
 1.3735    1.3071    1.2895    1.2866    1.2833    1.2825    1.2825    1.2623    1.2405    1.2186    1.2089    1.2089    1.2
 1.2248    1.2245    1.1829    1.1772    1.1772    1.1772    1.1772    1.1772    1.1772    1.1772    1.1772    1.1772    1.1
 1.1430    1.1430    1.1430    1.1430    1.1430    1.1430    1.1430    1.1430    1.1430    1.1430    1.1430    1.1430    1.1
 1.1430    1.1430    1.1430    1.1430    1.1612    1.1923    1.2358    1.2745    1.2781    1.2216    1.1735    1.1735    1.1
 1.1735    1.1735    1.1735    1.1735    1.1735    1.1735    1.1735    1.1735    1.1735    1.1735    1.1735    1.1735    1.1
 1.1363    1.1344    1.1344    1.1344    1.1344    1.1387    1.1406    1.1451    1.1505    1.1661    1.1857    1.1857    1.2
 1.3405    1.3487    1.3555    1.3653    1.3753    1.3846    1.4235    1.4311    1.4311    1.4311    1.4684    1.4684    1.4
 1.4684    1.4684    1.4684    1.4684    1.4684    1.4684    1.4684    1.4684    1.4684    1.4684    1.4826    1.4826    1.4
 1.4826    1.4337    1.4337    1.4337    1.4337    1.4337    1.4337    1.4337    1.4337    1.4337    1.4337    1.4337    1.4
 1.3544    1.2356    1.2271    1.2271    1.2271    1.2271    1.2271    1.2271    1.2271    1.2271    1.2271    1.2271    1.2
 1.2271    1.2271    1.2271    1.2271    1.2769    1.3559    1.3588    1.3559    1.3559    1.2938    1.2599    1.2477    1.2
 1.0117    1.0117    1.0117    1.0117    1.0117    1.0117    1.0117    1.0117    1.0117    1.0117    1.0117    1.0117    1.0
 1.0117    1.0117    1.0117    1.0117    1.0117    1.0117    1.0117    1.0117    1.0117    1.0117    1.0561    1.1852    1.1
 1.1852    1.1852    1.1852    1.1852    1.1852    1.1852    1.1852    1.1852    1.1852    1.1852    1.1852    1.1852    1.1
 1.1852    1.1852    1.3087    1.3181    1.3181    1.3181    1.3181    1.3181    1.3181    1.3181    1.3181    1.4160    1.4
 1.5794    1.5933    1.5933    1.5571    1.5092    1.4270    1.4266    1.4266    1.4266    1.4266    1.4266    1.4266    1.4
 1.1768    1.1731    1.1731    1.0422    1.0371    1.0371    1.0371    1.0371    1.0371    1.0371    1.0371    1.0371    1.0
 1.0371    1.0371    1.0371    1.0371    1.0371    1.0371    1.0371    1.0371    1.0371    1.0371    1.0371    1.0371    1.0
 1.0371    1.0371    1.0371    1.0371    1.0875    1.0875    1.1051    1.1532    1.1532    1.1532    1.1776    1.3052    1.6
 1.5021    1.5021    1.5021    1.5021    1.5021    1.5021    1.5021    1.5021    1.5021    1.5021    1.5021    1.5021    1.5
 1.6142    1.6142    1.6142    1.6142    1.6142    1.6142    1.6190    1.6771    1.6973    1.6973    1.6973    1.6973    1.6
 1.4081    1.2689    1.1876    1.1167    1.0648    1.0154    0.9891    0.9813    0.9797    0.9797    0.9760    0.9760    0.9
 0.9758    0.9758    0.9758    0.9758    0.9758    0.9758    0.9758    0.9758    0.9758    0.9758    0.9758    0.9758    0.9
 0.9798    0.9798    0.9798    0.9798    0.9798    0.9798    0.9798    0.9802    0.9975    1.0306    1.0306    1.0306    1.0
```

References

[1] R. L. Schuster and L. M. Highland, "Impact of landslides and innovative landslide-mitigation measures on the natural environment," tech. rep., Geologic Hazards Team, U.S. Geological Survey, Denver, Colorado, U.S.A., 2004.

[2] F. C. Dai, C. F. Lee, J. Li, and Z. W. Xu, "Assessment of landslide susceptibility on the natural terrain of lantau island, hong kong," *Environmental Geology*, vol. 42, no. 2, pp. 214–223, 2002.

[3] D. K. Keefer, "Landslides caused by earthquakes," *Geological Society of America Bulletin*, vol. 95, no. 4, pp. 406–421, 1984.

[4] D. M. Cruden and D. J. Varnes, "Landslide types and processes," in *Special Report*, no. 247, pp. 36–75, Transportation Research Board, U.S. National Academy of Sciences, 1996.

[5] S. Collico, M. Arroyo, R. Urgeles, E. Gràcia, M. Devincenzi, and N. Pérez, "Probabilistic mapping of earthquake-induced submarine landslide susceptibility in the south-west iberian margin," *Marine Geology*, vol. 429, p. 106296, 2020.

[6] V. B. Svalova, V. B. Zaalishvili, G. P. Ganapathy, A. V. Nikolaev, and D. A. Melkov, "Landslide risk in mountain areas," *Geology and Geophysics of the South of Russia*, vol. 10, no. 2, pp. 110–127, 2019.

[7] O. Dewitte, A. Dille, A. Depicker, D. Kubwimana, J.-C. Maki Mateso, T. Mugaruka Bibentyo, J. Uwihirwe, and E. Monsieurs, "Constraining landslide timing in a data-scarce context: From recent to very old processes in the tropical environment of the north tanganyika-kivu rift region," *Landslides*, vol. 18, no. 1, pp. 161–177, 2021.

[8] A. S. M. M. Kamal, F. Hossain, B. Ahmed, M. Z. Rahman, and P. Sammonds, "Assessing the effectiveness of landslide slope stability by analysing structural mitigation measures and community risk perception," *Natural Hazards*, vol. 117, no. 3, pp. 2393–2418, 2023.

[9] A. Sbihi, M. Mastere, B. Benzougagh, V. Spalevic, P. Sestras, M. Radovic, S. B. Marković, L. Jaufer, and S. Kader, "Assessing landslide susceptibility in northern morocco: A geostatistical mapping approach in al hoceima-ajdir," *Journal of African Earth Sciences*, vol. 218, p. 105361, 2024.

[10] V. E. Nwazelibe, J. C. Egbueri, C. O. Unigwe, J. C. Agbasi, D. A. Ayejoto, and S. I. Abba, "Gis-based landslide susceptibility mapping of western rwanda: An integrated artificial neural network, frequency ratio, and shannon entropy approach," *Environmental Earth Sciences*, vol. 82, p. 439, 2023.

[11] J. B. Nsengiyumva, C. Mupenzi, and J. Zhang, "Gis-based landslide susceptibility modeling: A case study in western rwanda," *Geomatics, Natural Hazards and Risk*, vol. 9, no. 1, pp. 1032–1052, 2018.

[12] D. V. Griffiths and P. A. Lane, "Slope stability analysis by finite elements," *Geotechnique*, vol. 49, no. 3, pp. 387–403, 1999.

[13] D. T. Bui, B. Pradhan, O. Lofman, I. Revhaug, and O. B. Dick, "Landslide susceptibility mapping at hoa binh province (vietnam) using an adaptive neuro-fuzzy inference system and gis," *Computers and Geosciences*, vol. 45, pp. 199–211, 2011.

[14] R. Q. Huang and X. Fan, "The landslide story," *Nature Geoscience*, vol. 6, no. 4, pp. 325–326, 2017.

[15] S. Tinti and A. Manucci, "Gravitational stability computed through the limit equilibrium method revisited," *Geophysical Journal International*, vol. 164, pp. 1–14, 2006.

[16] J. M. Duncan, "State of the art: Limit equilibrium and finite-element analysis of slopes," *Journal of Geotechnical Engineering*, vol. 122, no. 7, pp. 577–596, 1996.

[17] A. W. Bishop, "The use of the slip circle in the stability analysis of slopes," *Geotechnique*, vol. 5, no. 1, pp. 7–17, 1955.

[18] W. Fellenius, "Calculation of the stability of earth dams," in *Transactions of the 2nd Congress on Large Dams*, pp. 445–462, 1936.

[19] M. of Agriculture and R. o. R. Animal Resources, "Updated environmental impact assessment report for karongi 12 and 13 site," May 2013. Updated by the Project Environmental Safeguard Team for the Land Husbandry, Water Harvesting, and Hillside Irrigation Project.

[20] D. Delvaux, J. Moeyersons, J. Lavreau, M. Fernandez, and F. Kervyn, "Tectonic significance of the karisimbi volcano and its influence on rwandan geology," *Journal of African Earth Sciences*, vol. 27, no. 2, pp. 369–382, 1998.

[21] H. V. Nhu, B. V. Duong, and H. D. Vu, "3d slopes stability modeling for landslide early warning design at halong city area," *Journal of Mining and Earth Sciences*, vol. 60, no. 6, pp. 31–41, 2019.

[22] S. Zhang and F. Wang, "Three-dimensional seismic slope stability assessment with the application of scoops3d and gis: A case study in atsuma, hokkaido," *Geoenvironmental Disasters*, vol. 6, no. 9, 2019. Open Access.

[23] S. Kumar, S. S. Choudhary, A. Burman, R. K. Singh, A. Bardhan, and P. G. Asteris, "Probabilistic slope stability analysis of mount st. helens using scoops3d and a hybrid intelligence paradigm," *Mathematics*, vol. 11, no. 18, p. 3809, 2023.

[24] M. Reid, S. Christian, D. Brien, and S. Henderson, *Scoops3D: Software to Analyze Three-dimensional Slope Stability Throughout a Digital Landscape*. Menlo Park: U.S. Geological Survey; Volcano Science Center, 2015.

[25] Rwanda Water Resources Board (RWB) and International Union for Conservation of Nature (IUCN), "The state of soil erosion control in rwanda," 2022. Funded by the Embassy of Kingdom of the Netherlands in Rwanda as part of the Embedding Integrated Water Resources Management in Rwanda project.

[26] M. Tuluka, "An estimate of the attenuation relationship for strong ground motion in the kivu province, western rift valley of africa," *Physics of the Earth and Planetary Interiors*, vol. 162, pp. 13–21, 2007.

[27] G. C. Ltd, "Soil investigation report: Construction of the proposed apartment at rubavu, western province, rwanda," tech. rep., Geo Consult Ltd, Kigali, Rwanda, April 2018. Prepared for EAACON LTD.

[28] N. I. of Statistics of Rwanda (NISR), "The fifth rwanda population and housing census, district profile: Karongi," September 2023.

[29] M. of Agriculture and A. R. (MINAGRI), "Environmental management plan for karongi 13-sub project," July 2009. Prepared by Green and Clean Solution Ltd.

[30] A. Depicker, G. Govers, L. Jacobs, B. Campforts, J. Uwihirwe, and O. Dewitte, "Interactions between deforestation, landscape rejuvenation, and shallow landslides in the north tanganyika–kivu rift region, africa," *Earth Surface Dynamics*, vol. 9, pp. 445–462, 2021.

[31] S. Mandal and R. Maiti, *Semi-Quantitative Approaches for Landslide Assessment and Prediction*. Springer Natural Hazards, Singapore: Springer, 2015.

[32] P. Thambidurai and T. N. Singh, eds., *Landslides: Detection, Prediction and Monitoring: Technological Developments*. Cham, Switzerland: Springer Nature Switzerland AG, 2023.